CMLS, Cell. Mol. Life Sci. 54 (1998) 171–178
1420-682X/98/020171-08 $ 1.50 + 0.20/0

CMLS Cellular and Molecular Life Sciences

NMR structures of the C-terminal end of human complement serine protease C1s

P. Gans[a], V. Rossi[b], C. Gaboriaud[c], I. Bally[b], J.-F. Hernandez[b], M. J. Blackledge[a] and G. J. Arlaud[b, *]

[a]Laboratoire de Résonance Magnétique Nucléaire, Institut de Biologie Structurale Jean-Pierre Ebel (CEA/CNRS), 41 Avenue des Martyrs, F-38027 Grenoble Cedex 1 (France)
[b]Laboratoire d'Enzymologie Moléculaire, Institut de Biologie Structurale Jean-Pierre Ebel (CEA/CNRS), 41 Avenue des Martyrs, F-38027 Grenoble Cedex 1 (France), Fax +33 476885494, e-mail: arlaud@ibs.ibs.fr
[c]Laboratoire de Cristallogénèse et Cristallographie des Protéines, Institut de Biologie Structurale Jean-Pierre Ebel (CEA/CNRS), 41 Avenue des Martyrs, F-38027 Grenoble Cedex 1 (France)

Received 19 November 1997; accepted 24 November 1997

Abstract. Synthetic peptides derived from the C-terminal end of the human complement serine protease C1s were analysed by circular dichroism and nuclear magnetic resonance (NMR) spectroscopy. Circular dichroism indicates that peptides 656-673 and 653-673 are essentially unstructured in water and undergo a coil-to-helix transition in the presence of increasing concentrations of trifluoroethanol. Two-dimensional NMR analyses performed in water/trifluoroethanol solutions provide evidence for the occurrence of a regular α-helix extending from Trp659 to Ser668 (peptide 656-673), and from Tyr656 to Ser668 (peptide 653-673), the C-terminal segment of both peptides remaining unstructured under the conditions used. Based on these and other observations, we propose that the serine protease domain of C1s ends in a 13-residue α-helix (656Tyr-Ser668) followed by a five-residue C-terminal extension. The latter appears to be flexible and is probably locked within C1s through a salt bridge involving Glu672.

Key words. Complement; C1s; serine proteases; peptide synthesis; NMR structure.

Human C1s is a highly specific modular protease that is responsible for the enzymic activity of C1, the initial component of the classical pathway of the complement system [1, 2]. Its catalytic region, involved in the recognition and limited proteolysis of complement components C4 and C2, comprises two contiguous 'complement control protein' (CCP) modules connected, through a short intermediary segment, to a serine protease domain. Although no information about the crystallographic structure of C1s is presently available, recent studies based on chemical cross-linking and homology modelling [3] have led to a three-dimensional model of the assembly of the C-terminal part of the catalytic region, comprising the second CCP module, the intermediary segment, and the serine protease domain. This model is based, in large part, on the occurrence of an ionic bond between Glu672, the penultimate residue of the serine protease domain, and Lys405, in the second CCP module.

A major uncertainty of this model arises from the structure of the C-terminal end of the serine protease domain which, based upon homology with serine proteases of known structure [4], was initially simply assumed to form a continuous α-helix. However, compared with the corresponding region of classical serine proteases such as trypsin, chymotrypsin and elastase, the C-terminal end of C1s is prolonged by a six-residue extension which contains a proline residue and is therefore unlikely to adopt an α-helical conformation. Indeed, recent structural studies on blood coagulation

* Corresponding author.

factor Xa, another serine protease featuring a C-terminal extension of the same length as C1s, indicate that this segment does not fold as an α-helix [5]. These considerations prompted us to further investigate the structure of the C-terminal end of the C1s serine protease domain by means of circular dichroism (CD) and nuclear magnetic resonance (NMR) structural studies performed on synthetic peptides derived from this region. Our data are consistent with the occurrence of a 13-residue α-helix followed by a nonhelical 5-residue C-terminal extension.

Materials and methods

Peptide synthesis. Peptides 653Val-Lys-Asn-Tyr-Val-Asp-Trp-Ile-Met-Lys-Thr-Met-Gln-Glu-Asn-Ser-Thr-Pro-Arg-Glu-Asp673, 656Tyr-Asp673 and 665Gln-Asp673, corresponding to different segments from the C-terminal end of the human C1s serine protease domain, were synthesized chemically by the stepwise solid-phase method [6], using an Applied Biosystems 430A automated synthesizer. Synthesis was performed on a phenylacetamidomethyl resin, and the *tert*-butyloxycarbonyl group was used for protection of the *N*-α-amino group of all amino acids. Protecting groups for amino acid side chains were as follows: Arg (mesitylene sulfonyl), Asp (cyclohexyl), Glu (benzyl), Lys (2-chlorobenzyl oxycarbonyl), Ser (benzyl), Thr (benzyl), Trp (formyl), Tyr (bromobenzyloxycarbonyl). Met was used without side-chain protection. All couplings were performed by the dicyclohexylcarbodiimide/1-hydroxybenzotriazole method, using *N*-methylpyrrolidone and dimethylsulphoxide as coupling solvents, according to the protocol defined by Applied Biosystems.

Deprotection and cleavage of the peptides from the resin was performed with trifluoromethane sulphonic acid and removal of the protecting formyl group from tryptophan was achieved by treatment of the peptide for 5 min at 0 °C with 1 M ethanolamine in 6 M guanidine-HCl, pH 11. Reduction of methionine sulphoxide generated during synthesis was achieved by treatment of the peptide with *N*-methylmercaptoacetamide as described previously [7]. The peptides were purified by preparative reverse-phase high-pressure liquid chromatography (HPLC) on a 30-nm Vydac C18 column (2.2 cm × 25 cm, 10 μm) using a 30-min linear gradient of acetonitrile (5–60%) in 0.1% trifluoroacetic acid.

Mass spectrometry. Fast-atom bombardment mass-spectrometry analyses were carried out on a VG analytical ZAB-SE double-focusing mass spectrometer, as described previously [8]. Peptides were dissolved in 5% acetic acid, and thioglycerol was used as the matrix.

Circular dichroism. Spectra were recorded at 25 °C between 180 and 250 nm on a Jobin-Yvon CD6 spectrodichrograph, using a quartz cell of 1-mm path length, with a 5-s integration time for each 0.2-nm step. Peptides were dissolved at 40 μg/ml in 2,2,2-trifluoro-ethanol (TFE)/water mixtures containing 0–50% (v/v) TFE. For each measurement, the baseline was corrected for the corresponding solvent mixture. Estimation of the helical content of peptides was based on the mean residue ellipticity at 222 nm ($-32{,}000$ deg × cm^2 × dmol^{-1}) reported for a 17-residue α-helical peptide [9].

NMR spectroscopy. Peptides 656Tyr-Asp673 and 653 Val-Asp673 were dissolved at a final concentration of 12 mM in mixtures containing 150 μl of 50 mM phosphate buffer, pH 6.8, 50 μl of deuterated water, 300 μl of CF_3CD_2OD (peptide 656Tyr-Asp673) and 250 μl of 50 mM phosphate buffer, pH 6.8, 50 μl of deuterated water, 200 μl of CF_3CD_2OD (peptide 653Val-Asp673). Samples were sealed in a 5-mm diameter NMR tube under argon. For H/D exchange experiments, the solution of peptide 656Tyr-Asp673 was freeze-dried, then amide proton exchange rates in D_2O were monitored over a day period by recording a series of one-dimensional spectra every 30 min at 10 °C immediately after dissolving the peptide in 40% D_2O/60% CF_3CD_2OD.

NMR spectra were recorded at 10 °C on a Bruker AMX spectrometer operating at a 600-MHz proton frequency. Chemical shifts were reported relative to the water resonance fixed at 4.92 ppm. ^{1}H 2D spectra, double quantum filtered correlation spectroscopy (DQF-COSY) [10], total correlation spectroscopy homonuclear Hartman–Hahn spectroscopy (TOCSY/HOHAHA) [11,12], and nuclear Overhauser correlation spectroscopy (NOESY) [13–14] spectra were recorded in the States-time-proportional-phase incrementation (TPPI) mode [15]. Water resonance was attenuated by means of a coherent low-power ($\gamma B_2/2\pi = 50$ Hz) presaturation during the relaxation delay. For NOESY and TOCSY experiments, this presaturation was further combined with a 'jump and return' read pulse [16]. The isotropic mixing time was set to 55 ms, and the NOE mixing time to 75 and 150 ms. 2D spectra were collected as 512 (t_1) and 2048 (t_2) complex point time-domain matrix with spectral widths of 6250 and 6241 Hz, respectively. Thirty-two scans were used per t_1 increment. They were transformed after zero-filling in the F_1 dimension, into 1024 and 1024 real points in F_1 and F_2 dimension frequency-domain spectra using FELIX software version 2.3 (Biosym Technologies/Molecular Simulation Inc., San Diego, CA, USA).

NMR-derived geometrical bounds. Interproton distance restraints were derived from NOESY experiments acquired at 10 °C with 75- and 150-ms mixing times, in 40% H_2O/60% CF_3CD_2OD. NOE intensities were classified as strong, medium, weak or very weak (corre-

sponding upper-distance limits were 2.8, 3.8, 5.0 and 6.0 Å, respectively). These distances were calibrated using the NH_E–NH_Z distances of Gln665 and Asn667 as references. Unresolved protons were replaced by pseudo-atoms, and an appropriate correction was applied to the measured distance [17]. Nonstereospecifically assigned but spectroscopically resolved protons were allowed to float between the two prochiral positions during the simulated annealing protocols. All peptide bonds were maintained in a *trans* conformation.

Structure calculations. Structure calculations were performed using DISCOVER (version 2.9.7, 1993) from Biosym Technologies interfaced to the INSIGHT II program (version 2.3.0, 1993) for visualization and data analysis. The AMBER4 force field [18] was used for all calculations except for the simulated annealing protocols, in which a simple quartic nonbond term was employed. The protocol was divided into two parts: in the first stage, a simulated annealing procedure was used to provide the broadest possible sampling of the conformational space. Cartesian coordinates were randomized at the start of each run. In the initial stages the calculation was dominated by the experimental constraints (the force constant for the semiparabolic distance constraints was 50 kcal mol^{-1} $Å^{-2}$). Experimental, covalent and nonbond terms were augmented gradually during the high-temperature (1000 K) period of the simulation before final cooling to 100 K [19]. The nonbond terms were reduced to a simple repulsive quartic term to facilitate sampling of a large conformational space, and the Coulombic interaction was ignored in this first step. The total simulation time was 62 ps. These approximate structures were then refined by restrained molecular dynamics calculation using the full AMBER4 force-field description (including Coulomb and van der Waals terms). Solvent effects were approximated using reduced charges for the polar residues [20]. The molecule was equilibrated at a temperature of 750 K, using a distance constraint of 25 kcal mol^{-1} $Å^{-2}$, allowed to evolve during a period of 11 ps and then cooled over a period of 3.5 ps to 300 K, where the molecule was again allowed to evolve over 12 ps. The step size for calculation of velocities was 1 fs. The final structures were energy-minimized using the same force field with a conjugate gradient algorithm, and these structures were used for analysis.

Results

Chromatographic analysis of the purified synthetic peptides by analytical reverse-phase HPLC indicated that they were homogeneous. This was confirmed by fast-atom bombardment mass spectrometry analysis, which also showed that all peptides had the expected sequence, yielding mass values of 2584.8 ± 0.4 Da (peptide 653Val-Asp673), 2243.2 ± 0.4 Da (peptide 656Tyr-Asp673) and 1074.0 ± 0.4 Da (peptide 665Gln-Asp673) (calculated average mass values were 2584.9, 2243.5 and 1075 Da, respectively).

CD studies. Far-ultraviolet (UV) spectra of the C1s C-terminal peptide 656Tyr-Asp673 were recorded in water as well as in different water–TFE mixtures at 25 °C (fig. 1A). The spectrum in water exhibited a mean residue ellipticity at 222 nm of approximately -7000 deg × cm^2 × $dmol^{-1}$, indicating a low but nevertheless detectable helical content. Increasing the TFE concentration gradually increased the α-helix content, as shown by the progressive appearance of characteristic minima at 208 and 222 nm. The isodichroic point at

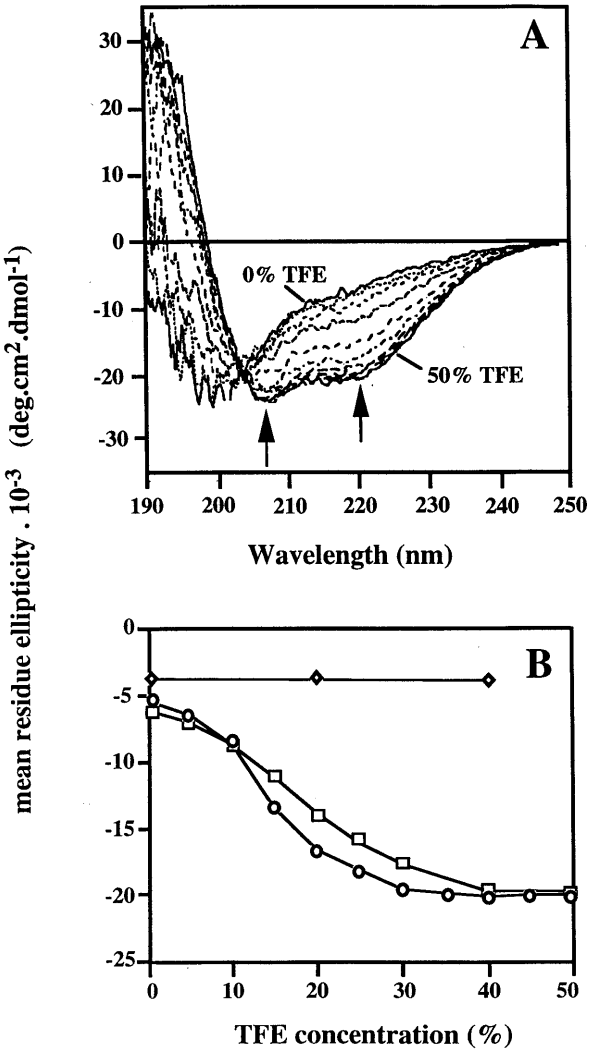

Figure 1. (*A*) Far-UV CD spectra of the C1s C-terminal peptide 656Tyr-Asp673 in the presence of increasing concentrations of TFE in water. The arrows indicate the minima at 208 and 222 nm. (*B*) Plots of the mean residue ellipticity at 222 nm as a function of TFE concentration. (◇) peptide 665Gln-Asp673; (□) peptide 656Tyr-Asp673; (○) peptide 653Val-Asp673.

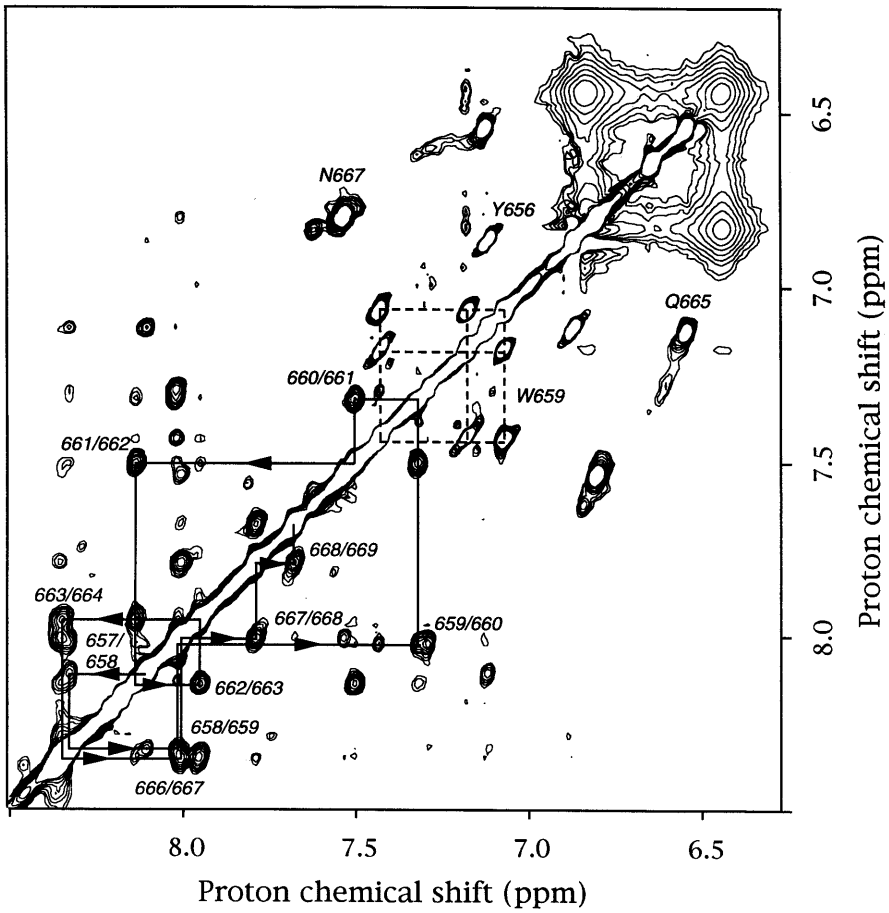

Figure 2. Amide proton–amide proton region of the NOESY spectrum (600 MHz, 150 ms mixing time) of peptide 656Tyr-Asp673 (12 mM) in 40% H_2O/60% TFE at 10 °C. Sequential connectivities are arrowed from residues Val657 to Thr669.

203–204 nm was indicative of a two-state coil-to-helix transition. As judged from the plot of the mean residue ellipticity at 222 nm as a function of TFE concentration (fig. 1B), the α-helix content reached a plateau at 40–50% TFE, with a value of about $-20{,}000$ degree $\times$ cm^2 $\times$ dmol^{-1}, consistent with about two-thirds of the 18 amino acids being in helical conformation.

CD analysis of the larger peptide 653Val-Asp673 under the same conditions yielded comparable results, indicating that the peptide was essentially disordered in water and acquired α-helical conformation in the presence of increasing TFE concentrations. However, the helix content reached a plateau at a slightly lower TFE concentration (30–40%) (fig. 1B), with mean residue ellipticity at 222 nm comparable to that observed for peptide 656Tyr-Asp673.

CD analysis was also performed on peptide 665Gln-Asp673, corresponding to the C-terminal end of the preceding two peptides. In that case, the spectrum in water showed a mean residue ellipticity at 222 nm of about -4000 deg $\times$ cm^2 $\times$ dmol^{-1}, which remained unchanged upon addition of increasing amounts of TFE up to 40% (fig. 1B). These data strongly suggested that the ability of the larger peptides 653Val-Asp673 and 656Tyr-Asp673 to adopt helical conformations in water–TFE mixtures was essentially a property of their N-terminal end. Further structural characterization by NMR spectroscopy was therefore performed only on peptides 656Tyr-Asp673 and 653Val-Asp673.

NMR spectroscopy studies. The NMR sequence-specific proton assignment [17] of peptide 656Tyr-Asp673 was obtained in a straightforward manner in 40% H_2O/60% CF_3CD_2OD at 10 °C. Figure 2 shows a representative part of the NOESY spectrum obtained under these conditions. NOE correlations as well as $^3J_{HN\alpha}$ spin–spin coupling analysis and chemical shift index [21] provided strong evidence for α-helix formation (fig. 3A). In good agreement with the estimate based on CD analysis, the medium-range NOEs together with the chemical shift index and $^3J_{HN\alpha}$ values were consistent with the presence of a helix spanning 10 amino acid residues, from Trp659 to Ser668. Some of the NOE correlations in this

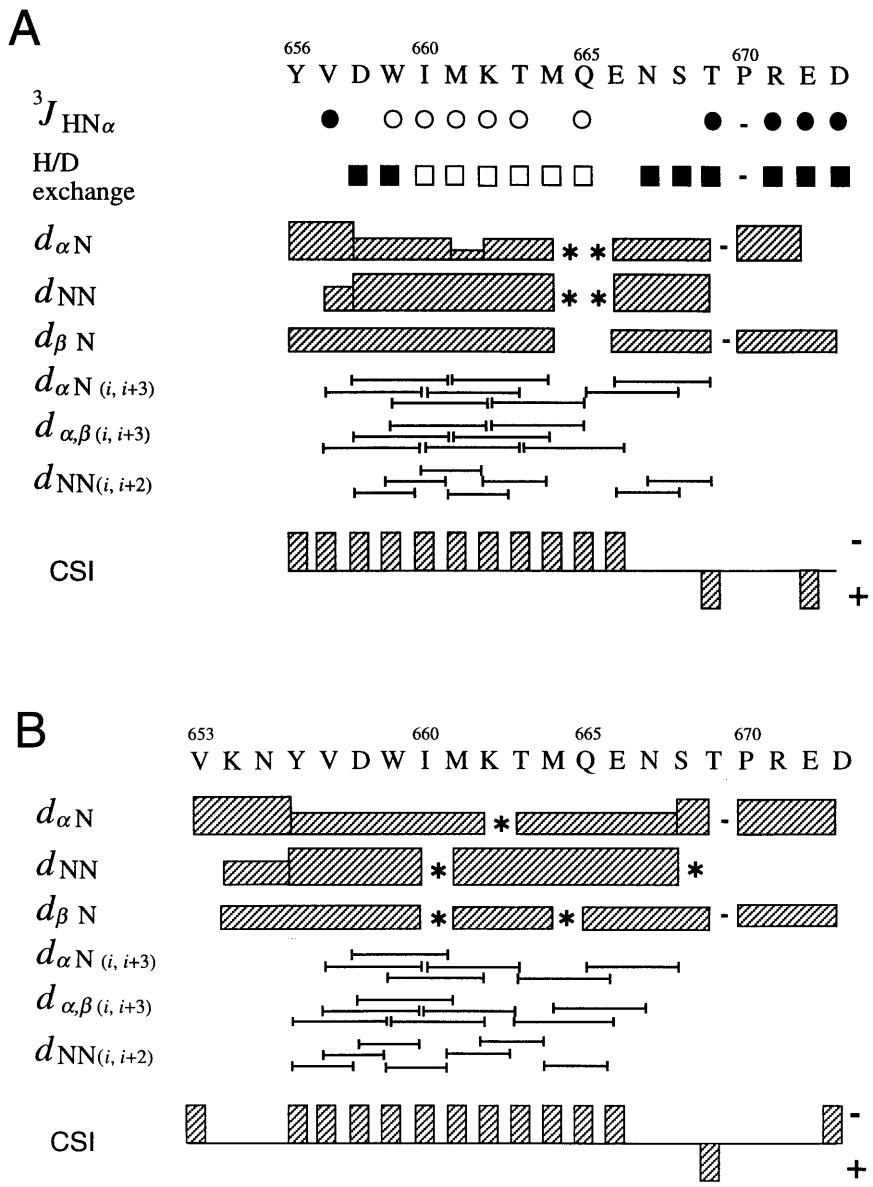

Figure 3. Summary of the sequential NOE connectivities involving NH, $C^{\alpha}H$, and $C^{\beta}H$. (*A*) Peptide 656Tyr-Asp673 analysed at 10 °C with a 150-ms mixing time in 40% H_2O/60% CF_3CD_2OD; (*B*) peptide 653Val-Asp673 analysed at 10 °C with a 150-ms mixing time in 60% H_2O/40% CF_3CD_2OD. NOEs are classified as strong, medium and weak according to the height of the hatched bar under the peptide sequence. Asterisks indicate a spectral overlap precluding observation of the NOE. Open and filled circles indicate $^3J_{HN\alpha}$ spin–spin coupling constants estimated from the COSY and TOCSY spectra to be less than 5 Hz and greater than 6 Hz, respectively. Open squares indicate amide protons present in one-dimensional spectra or in TOCSY spectra after 4 h of H/D exchange, and filled squares indicate protons absent after this period. The chemical shift index (CSI) represents the difference between the $C^{\alpha}H$ chemical shift of a residue and the mean value of the random-coil $C^{\alpha}H$ chemical shift for this particular residue [21]. Positive and negative bars indicate downfield and upfield shifts, respectively, of more than 0.1 ppm. The residue numbering used is that of the intact C1s protein.

region are missing because of the spectral overlap of the H^N resonances of residues Met664, Gln665 and Glu666 (fig. 3A). Quantification of the sequential NOE correlations within the C-terminal end of the peptide was made difficult because of the overlap of the H^N resonances of Arg671, Glu672 and Asp673. However, the qualitatively high $d_{\alpha N}$ values, the absence of $d_{\alpha,\beta(i,i+3)}$ and $d_{\alpha N(i,i+3)}$ connectivities, together with the chemical shift index and $^3J_{HN\alpha}$ values, clearly precluded an extension of the helical conformation beyond Ser668. Also, the occurrence of strong $d_{\alpha\delta}$ correlations between Thr669 and Pro670 indicated that the peptide bond was in a *trans* conformation. Finally, it should be mentioned that H/D exchange experiments allowed observation, after 4 h, of the amide protons from Ile660 to Gln665 (fig. 3A), indicating that the helical conformation was stable over this period.

Table 1. Structural statistics for the 34 structures of the C1s C-terminal peptide 656Tyr-Asp673 determined at 10 °C in 60% TFE/40% H_2O.

Structural statistics	34 structures
Cartesian coordinate r.m.s.d. (Å)*	
Residues 656-673	1.76 ± 0.28
Residues 659-668	0.15 ± 0.06
Residues 669-673	2.00 ± 0.12
Mean number of distance restraints violations per structure	
>0.40 Å	0
>0.30 Å	0.1
>0.20 Å	0.4 ± 0.7
>0.10 Å	5.8 ± 1.7
Mean number of distance restraints violations per structure in residues 659–668	
>0.40 Å	0
>0.30 Å	0.1
>0.20 Å	0.2
>0.10 Å	2.5 ± 1.2
AMBER potential energies†	
F_{total} (kcal mol^{-1})	-250.4 ± 10.2
$F_{Coulombic}$ (kcal mol^{-1})	-260.8 ± 9.5
E_{L-J} (kcal mol^{-1})	-37.4 ± 4.3
E_{exp} (kcal mol^{-1})	5.5 ± 1.2

*Mean r.m.s.d. values were calculated vs. the averaged geometric coordinates of the 34 structures using (N, C^{α}, C, O) backbone atoms.

†$F_{Coulombic}$ is the coloumbic energy contribution to F_{total}. E_{L-J} is the value of the Lennard-Jones–van der Waals energy function calculated by DISCOVER using the AMBER force field [18]. E_{exp} is calculated using a force constant of 25 kcal mol^{-1} Å^{-2}.

A set of 244 geometrical constraints, including 128 sequential and 111 medium-range upper-bound distances, was derived from the NOESY spectra. Only five intraresidue distance restraints were used in the structure calculation procedure. Dihedral constraints were not used for the calculation, as $^3J_{HN\alpha}$ coupling constants could only be qualitatively estimated from the spectra but not precisely measured. Seventeen structures were calculated in the first stage of simulated annealing, and each of them was used to generate two structures in the second stage of restrained molecular dynamics. The structural statistics are summarized in table 1. Figure 4 shows the superimposition of the 34 structures on the backbone atoms from the residues 659 to 668. The root-mean-square deviation (r.m.s.d.) value of these atoms is 0.15 ± 0.06 Å, a value which represents only a measure of the definition of the minimum in the conformational space sampled by the structure calculation algorithm, but not the amplitude of any dynamic process. The structures exhibit a regular α-helix conformation from Trp659 to Ser668, and the N-terminal end 656Tyr-Asp658, although not α-helical, also shows a preferential structure. In contrast, the C-terminal segment, from Thr669 to the end, is highly disordered, although preferential orientations can be observed on the side opposite to Ile660, Met664 and Asn667 (fig. 4). NMR sequence-specific proton assignment of the larger peptide 653Val-Asp673 was obtained in 60% H_2O/40% CF_3CD_2OD at 10 °C. As summarized in figure 3B, NOE correlations as well as chemical shift index [21] provided clear evidence for α-helix formation from Tyr656 to Ser668 (fig. 3B) under these conditions. As observed in the case of peptide 656Tyr-Asp673, the C-terminal part, from Thr669 to Asp673, is unstructured. The observations of NOE correlations between Thr669 and Arg671 indicate that the C-terminal part of this peptide adopts the same preferential orientations as described above for peptide 656Tyr-Asp673.

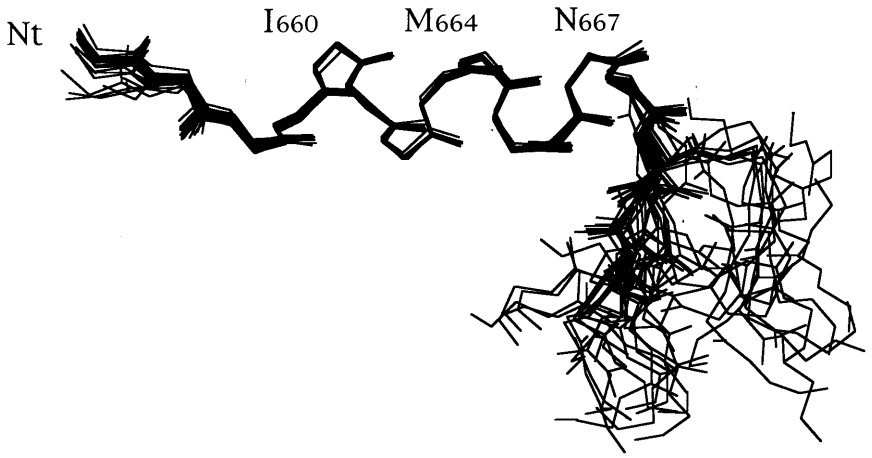

Figure 4. R.m.s. superimpositions of the (N, C^{α}, C, O) atoms of residues 659-668 of 34 calculated structures of the C-terminal 656Tyr-Asp673 peptide from the serine protease domain of C1s. The structures were calculated from the geometrical boundaries derived from the NMR experiments performed at 10 °C in 40% H_2O/60% CF_3CD_2OD. Only backbone atoms are represented. Nt, N-terminal end; Ct, C-terminal end.

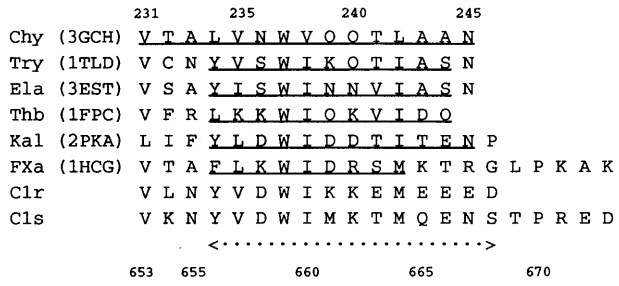

Figure 5. Alignment of the C-terminal sequences of various serine proteases. Underlined is the extent of unequivocal α-helical secondary structure in the known X-ray structures [5, 24–28], which was controlled with the PROCHECK program [29]. ($<\cdots\cdots>$), proposed length of the C-terminal α-helix in C1s; Chy, bovine chymotrypsin; Try, bovine trypsin; Ela, porcine elastase; Thb, human thrombin; FXa, human coagulation factor Xa. PDB codes are indicated for the available X-ray structures. The numberings shown are those of chymotrypsin and C1s.

Discussion

Although the mechanism of action of TFE remains poorly understood, its ability to induce or enhance the helicity of peptides in water solutions has been widely demonstrated, and it is generally considered that TFE stabilizes α-helices in peptides possessing intrinsic helical propensity [22, 23]. On the other hand, the occurrence of an α-helix in the C-terminal region of serine proteases is a well-established feature shared by this family of proteins. Therefore, our observation that TFE promotes formation of stable helical structures from residues Trp659 to Ser668 and Tyr656 to Ser668 in peptides 656-673 and 653-673, respectively, strongly suggests that segment 656Tyr-Ser668 forms an α-helix in intact C1s. Comparison of available 3D structures of serine proteases (fig. 5) reveals that the C-terminal α-helix, which comprises between 9 residues (in coagulation factor Xa) and 15 residues (in chymotrypsin), starts at the level of residue 656 of C1s in all proteases but chymotrypsin. In that case, however, a bend occurs at residue 233, and the canonical helix only starts at residue 234, which is homologous to residue 656 in C1s (fig. 5). The fact that residues 656Tyr-Val-Asp658 do not adopt a helical conformation in the shorter peptide 656-673 is likely due to their location at the N-terminal tip of the peptide, which may exert a destabilizing effect. In the same way, residues 665Gln-Glu-Asn-Ser668 are an integral part of the helix in both peptides 653-673 and 656-673 but, as judged from our CD analysis, show no significant helical structure in peptide 665-673. On the basis of these observations, it is highly likely that the C-terminal helix in intact C1s encompasses 13 residues, from Tyr656 to Ser668. By analogy, it may be hypothesized that most, if not all, of the C-terminal 13 residues of C1r, the other serine protease of C1, form a regular α-helix (fig. 5).

The NMR analyses of both peptides 653-673 and 656-673 clearly preclude the occurrence of a helical structure from Thr669 to Asp673. As recently shown for the C-terminal extension of factor Xa [5], it is therefore very likely that the very C-terminal segment of C1s, 669Thr-Asp673, does not fold as the continuity of the preceding α-helix. The NMR-derived model shown on figure 4 suggests that this segment is flexible and able to adopt a variety of conformations. In view of the intramolecular interaction shown to occur between the serine protease domain and the second CCP module of C1s [3], a likely hypothesis is that its final orientation within C1s is driven by long-range interactions with the remainder of the protein, and stabilized mainly by the salt bridge that takes place between Lys405, in the second CCP module, and Glu672, the penultimate residue of the protease.

Acknowledgements. This work was supported by the Commissariat à l'Energie Atomique and the Centre National de la Recherche Scientifique. We are indebted to Biosym Technologies for the use of the FELIX software. We thank D. Marion for critical reading of the manuscript. This is publication no. 444 from the Institut de Biologie Structurale Jean-Pierre Ebel.

1 Schumaker V. N., Zavodszky P. and Poon P. H. (1987) Activation of the first component of complement. Annu. Rev. Immunol. **5:** 21–42
2 Arlaud G. J., Colomb M. G. and Gagnon J. (1987) A functional model of the human C1 complex. Immunol. Today **8:** 106–111
3 Rossi V., Gaboriaud C., Lacroix M., Ulrich J., Fontecilla-Camps J. C., Gagnon J. et al. (1995) Structure of the catalytic region of human complement protease C1s: study by chemical cross-linking and three-dimensional homology modeling. Biochemistry **34:** 7311–7321
4 Greer J. (1990) Comparative modeling methods: application to the family of the mammalian serine proteases. Proteins **7:** 317–334
5 Padmanabhan K., Padmanabhan K. P., Tulinsky A., Park C. P., Bode W., Huber R. et al. (1993) Structure of human Des (1-45) Factor Xa at 2.2 Å resolution. J. Mol. Biol. **232:** 957–966
6 Barany G. and Merrifield R. B. (1980). In: The Peptides, vol. 2, pp. 1–284, Gross E., Meienhofer J. (eds), Academic Press, New York
7 Girardet J.-L., Bally I., Arlaud G. J. and Dupont Y. (1993) Localization of a putative magnesium-binding site within the cytoplasmic domain of the sarcoplasmic reticulum Ca^{2+}-ATPase. Eur. J. Biochem. **217:** 225–231
8 Thielens N. M., Van Dorsselaer A., Gagnon J. and Arlaud G. J. (1990) Chemical and functional characterization of a fragment of C1s containing the epidermal growth factor homology region. Biochemistry **29:** 3560–3578
9 Marqusee S., Robbins V. H. and Baldwin R. L. (1989) Unusually stable helix formation in short alanine-based peptides. Proc. Natl. Acad. Sci. USA **86:** 5286–5290
10 Rance M., Sørensen O. W., Bodenhausen G., Wagner G., Ernst R. R. and Wüthrich K. (1983) Improved spectral resolution in COSY ^{1}H NMR spectra of proteins via double quantum filtering. Biochem. Biophys. Res. Commun. **117:** 479–485
11 Braunschweiler L. and Ernst R. R. (1983) Coherence transfer by isotopic mixing: application to proton correlation spectroscopy. J. Magn. Reson. **53:** 521–528
12 Davis D. G. and Bax A. (1985) Assignment of complex ^{1}H NMR spectra via two-dimensional homonuclear Hartmann–Hahn spectroscopy. J. Am. Chem. Soc. **107:** 2820–2821

13 Jeener J., Meier B. H., Bachmann P. and Ernst R. R. (1979) Investigation of exchange processes by two-dimensional NMR spectroscopy. J. Chem. Phys. **71:** 4546–4553
14 Macura S., Hyang Y., Suter D. and Ernst R. R. (1981) A two-dimensional chemical exchange and cross-relaxation spectroscopy of coupled nuclear spins. J. Magn. Reson. **43:** 259–281
15 Marion D., Ikura M., Tschudin R. and Bax A. (1989) Rapid recording of 2D NMR spectra without phase cycling. Application to the study of hydrogen exchange in proteins. J. Magn. Reson. **85:** 393–399
16 Plateau P. and Guéron M. (1982) Exchangeable proton NMR without base-line distorsion, using new strong-pulse sequences. J. Am. Chem. Soc. **104:** 7310–7311
17 Wüthrich K. (1986) NMR of Proteins and Nucleic Acids, John Wiley, New York
18 Pearlman D. A., Case D. A., Caldwell J. C., Seibel G. L., Singh U. C., Weiner P. et al. (1991) Amber 4.0, University of California, San Francisco
19 Nilges M., Clore G. M. and Gronenborn A. M. (1988) Determination of three-dimensional structures of proteins from interproton distance data by dynamical simulated annealing from a random array of atoms. Circumventing problems associated with folding. FEBS Lett. **239:** 129–136
20 Blackledge M. J., Medvedeva S., Poncin M., Guerlesquin F., Bruschi M. and Marion D. (1995) Structure and dynamics of ferrocytochrome c-553 from *Desulfovobrio vulgaris* by NMR spectroscopy and restrained molecular dynamics. J. Mol. Biol. **245:** 661–681
21 Wishart D. S., Sykes B. D. and Richards F. M. (1991) Relationship between nuclear magnetic resonance chemical shift and protein secondary structure. J. Mol. Biol. **222:** 311–333
22 Rajan R. and Balaram P. (1996) A model for the interaction of trifluoroethanol with peptides and proteins. Int. J. Peptide Protein Res. **48:** 328–336
23 Kemmick J. and Creighton T. E. (1995) Effects of trifluoroethanol on the conformations of peptides representing the entire sequence of bovine pancreatic trypsin inhibitor. Biochemistry **34:** 12630–12635
24 Bartunik H. D., Summers L. J. and Bartsch H. H. (1989) Crystal structure of bovine beta-trypsin at 1.5 Å resolution in a crystal form with low molecular packing density. Active site geometry, ion pairs and solvent structure. J. Mol. Biol. **210:** 813–828
25 Birktoft J. J. and Blow D. M. (1972) Structure of crystalline α-chymotrypsin. V. The atomic structure of tosyl-α-chymotrypsin at 2 Å resolution. J. Mol. Biol. **68:** 187–240
26 Sawyer L., Shotton D. M., Campbell J. W., Wendell P. L., Muirhead H., Watson H. C. et al. (1978) The atomic structure of crystalline porcine pancreatic elastase at 2.5 Å resolution: comparisons with the structure of alpha-chymotrypsin. J. Mol. Biol. **118:** 137–208
27 Mathews I. I., Padmanabhan K. P., Ganesh V., Tulinsky A., Ishii M., Chen J. et al. (1994) Crystallographic structures of thrombin complexed with thrombin receptor peptides: existence of expected and novel binding modes. Biochemistry **33:** 3266–3279
28 Bode W., Chen Z., Bartels K., Kutzbach C., Schmidt-Kastner G. and Bartunik H. (1983) Refined 2 Å X-ray crystal structure of porcine pancreatic kallikrein A, a specific trypsin-like serine proteinase. Crystallization, structure determination, crystallographic refinement, structure and its comparison with bovine trypsin. J. Mol. Biol. **164:** 237–282
29 Laskowski R. A., MacArthur M., Moss D. S. and Thornton J. M. (1993) PROCHECK: a program to check the stereochemical quality of protein structures. J. Appl. Cryst. **26:** 283–291